

Supporting Information

Multiscale porous molybdenum phosphide of honeycomb structure for highly efficient hydrogen evolution

Mengjie Hou,¹ Xue Teng,¹ Jianying Wang,¹ Yangyang Liu,¹ Lixia Guo,¹ Lvlv Ji,¹ Chuanwei
Cheng² and Zuofeng Chen^{*,1}

¹Shanghai Key Lab of Chemical Assessment and Sustainability, School of Chemical Science
and Engineering, Tongji University, Shanghai 200092, China

²School of Physics Science and Engineering, Tongji University, Shanghai 200092, China

Experimental Section

Chemicals

Ammonia hydroxide ($\text{NH}_3 \cdot \text{H}_2\text{O}$, 28%), absolute ethanol ($\text{C}_2\text{H}_5\text{OH}$, $\geq 99.7\%$), hydrofluoric acid (HF, 40%w/w), silicon dioxide (SiO_2), ammonium molybdate tetrahydrate ($(\text{NH}_4)_6\text{Mo}_7\text{O}_{24} \cdot 4\text{H}_2\text{O}$, 99%), molybdenum trioxide (MoO_3 , 99.5%) and ammonium phosphate ($(\text{NH}_4)_2\text{HPO}_4$, 99%) were purchased from Macklin Chemical Regent Company. D (+)-glucose (99%) and tetraethyl orthosilicate (TEOS, 99.9%) were purchased from Aladdin Chemical

Regent Company. Nafion solution (5 wt% in a mixture of lower aliphatic alcohols and water) and 20 wt% Pt/C were purchased from Sigma-Aldrich Chemical Regent Company. Deionized (DI) water was used in all experiments. All reagents used in this experiment were analytical grade and used without further purification.

Instrumentation

Scanning electron microscopy (SEM) images, energy dispersive X-ray spectroscopy analysis (EDX) data and EDX mapping images were obtained at Hitachi S-4800 (Hitachi, Japan) equipped with a Horiba EDX system (X-max, silicon drift X-Ray detector). SEM images were obtained with an acceleration voltage of 3 kV, and EDX mapping images and EDX spectra were obtained with an acceleration voltage of 15 kV. The time for EDX mapping images is 15 min. Transmission electron microscopy (TEM) images, high resolution TEM (HRTEM) images and selected area electron diffraction (SAED) patterns were performed on a Tecnai G²F20 S-Twin electron microscopy with an accelerating voltage of 200 kV.

Powder X-ray diffraction (XRD) patterns were measured by Bruker D8 Focuss equipped with ceramic monochromatized Cu K α radiation (1.54178 Å). Corresponding work voltage and current is 40 kV and 40 mA, respectively. The scanning rate was 5° per min in 2θ and the scanning range was from 10°- 80°.

X-ray photoelectron spectroscopy (XPS) for elemental analysis was conducted on a Kratos Axis Ultra DLD X-ray Photoelectron Spectrometer using 60 W monochromated Mg K α radiation as the X-ray source for excitation. The 500 μm X-ray spot was used for XPS analysis. The base pressure in the analysis chamber was about 3×10^{-10} mbar. The C 1s peak (284.8 eV) was used for internal calibration. The peak resolution and fitting were processed by XPS Peak 4.1 software.

Brunauer-Emmett-Teller (BET) specific surface areas were measured by N₂ adsorption at 77 K using a volumetric unit (Micromeritics ASAP 2020). The samples loaded in a pre-weighted BET sample tube were degassed for 3 h at 200 °C prior to measurements. The pore size distribution was analyzed by the Barrett-Joyner-Halenda (BJH) method.

Thermogravimetric analysis (TGA) measurements of MoP@HCC materials were carried out on a TGA Q500 at temperatures from 20 to 800 °C with a ramping rate of 1 °C min⁻¹ under the high-purity air atmosphere.

Procedures

Preparation of monodisperse silica nanospheres. Monodisperse silica nanospheres were synthesized as templates by the Stöber method.¹ The preparation of silica spheres involves the ammonia-catalyzed hydrolysis and condensation of TEOS in an aqueous ethanol solution. Briefly, 250 mL of absolute ethanol, 20 mL of DI water, and 15 mL of 28% NH₃•H₂O were mixed

and stirred together for 1 h at room temperature. Subsequently, 15 mL of TEOS was added into the solution quickly. After stirring at room temperature for 6 h, the monodisperse silica nanospheres were collected by centrifugation. Finally, the white precipitate was washed with ethanol three times and air-dried at 50 °C overnight.

Preparation of honeycomb carbon (HCC). For the synthesis of HCC, typically, 0.5 g glucose was first added into 50 mL DI water in 500 mL beaker, and ultrasonically treated for 5 min. Then 1.0 g monodisperse silica nanospheres were added into the dispersion under vigorous stirring, and kept stirring at 70 °C until DI water were evaporated. The obtained SiO₂@glucose nanocomposites were collected, dried and grinded for 10 min. Then, SiO₂@glucose nanocomposites were placed in a porcelain boat carbonized under an Ar atmosphere at 900 °C for 3 h with a heating rate of 5 °C min⁻¹, which produced SiO₂@C. After etching out SiO₂ with a 10% HF solution for 24 h and being washed for several times with DI water, honeycomb carbon (HCC) was obtained.

Preparation of MoP@HCC. This catalyst material is prepared by a weight ratio of HCC: (NH₄)₆Mo₇O₂₄•4H₂O = 1: 2. First, 0.18 g (NH₄)₆Mo₇O₂₄•4H₂O was first added into 50 mL absolute ethanol in 100 mL beaker, and stirred together for 2 h at room temperature. Then 0.09 g HCC was added into the dispersion under vigorous stirring. After stirring at room temperature

for 24 h, the mixtures were collected by centrifugation, washed with absolute ethanol for several times and subject to freeze-drying. The as-obtained $(\text{NH}_4)_6\text{Mo}_7\text{O}_{24}@\text{HCC}$ were then placed in a porcelain boat, where ammonium phosphate was separately placed in the same boat with its mass twenty times of $(\text{NH}_4)_6\text{Mo}_7\text{O}_{24}@\text{HCC}$. The porcelain boat containing $(\text{NH}_4)_6\text{Mo}_7\text{O}_{24}@\text{HCC}$ and ammonium phosphate were placed in a tube furnace, and ammonium phosphate was in front of $(\text{NH}_4)_6\text{Mo}_7\text{O}_{24}@\text{HCC}$ in the Ar/H₂ blowing direction. After being annealed at 850 °C for 4 h with a heating rate of 2 °C min⁻¹, and cooling down to room temperature, the MoP@HCC catalyst was obtained. Other catalyst materials with weight ratios of HCC: $(\text{NH}_4)_6\text{Mo}_7\text{O}_{24}\cdot 4\text{H}_2\text{O}$ = 1:1, 1:1.5, 1:2.5 and 1:3 were also prepared by the same procedure and named as MoP@HCC-1, MoP@HCC-2, MoP@HCC-3, MoP@HCC-4, respectively. The contrast sample of the MoP/C composite was prepared by the same method with commercial silicon dioxide to substitute the as-prepared monodisperse silica nanospheres.

Preparation of bulk MoP. In a typical procedure, 50 mg MoO₃ and 1000 mg (NH₄)₂HPO₄ were grinded to powders and then placed in the porcelain boat. The boat was then heated at 850 °C under H₂/Ar for 8 h with a heating rate of 2 °C min⁻¹. After the temperature was cooled down to room temperature, the black powder was dispersed in 10 % HF solution for 24 h and washed

for several times with DI water. Finally, the resultant material was dried under vacuum at 100 °C for later HER test.

Preparation of MoO₂@HCC. The synthetic procedure of MoO₂@HCC was the same as that for MoP@HCC, except that the H₂/Ar was replaced by Ar.

Preparation of working electrodes. Catalyst ink was prepared by dispersing 4 mg of catalyst into 1 mL of water/ethanol (v/v = 4:1) solvent containing 80 μL of 5 wt% Nafion and sonicated for at least 30 min to form a homogeneous ink. Then 5 μL of the catalyst ink (containing 18.5 μg of catalyst) was loaded onto a glassy carbon electrode of 3 mm in diameter (loading ca. 0.26 mg cm⁻²) and dried at room temperature.

Electrochemical measurements. All electrochemical measurements were conducted using a CHI660E electrochemical workstation (CH Instruments, China) in a typical three-electrode setup with an electrolyte solution of 0.5 M H₂SO₄ solution at room temperature. Catalyst samples were loaded on the glassy carbon electrode (GCE, 0.07 cm² in area) as the working electrode, and a graphite rod was used as the counter electrode, and a saturated calomel electrode (SCE) was used as the reference electrode, respectively. Before the electrochemical tests, the fresh working electrode was cycled 50 times to stabilize the current and linear sweep voltammetry (LSV) measurement was conducted in a N₂-saturated 0.5 M H₂SO₄ solution with a scan rate of 5 mV

s⁻¹. The Tafel slope was obtained from the LSV plot using a linear fit applied to points in the Tafel region. The durability of the catalyst was tested in 0.5 M H₂SO₄ by electrolysis at a controlled potential of -0.14 V. Additionally, cyclic voltammograms (CV) were obtained around the open circuit potential (OCP) with sweep rates of 40, 60, 80, 100, 120, 140, 160 and 180 mV s⁻¹.

All the potentials reported in our work are expressed vs. the Reversible Hydrogen Electrode (RHE) with iR correction where the R was referred to the ohmic resistance arising from the electrolyte/contact resistance of the setup, measured prior to the experiment. In 0.5 M solution H₂SO₄, E (RHE) = E (SCE) + 0.273 V. Electrochemical impedance spectroscopy (EIS) measurements were carried out in the frequency range of 100 kHz – 0.01 Hz with an amplitude of 5 mV at the open-circuit voltage.

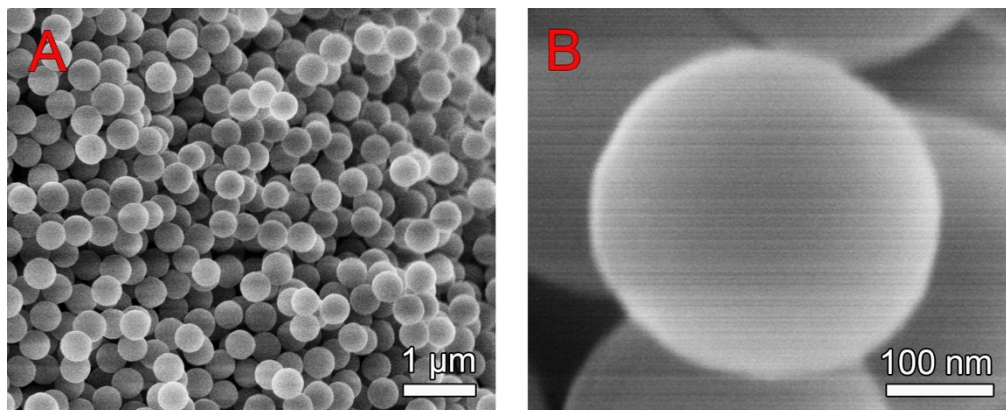


Figure S1. (A, B) SEM images of as-prepared SiO₂ nanospheres

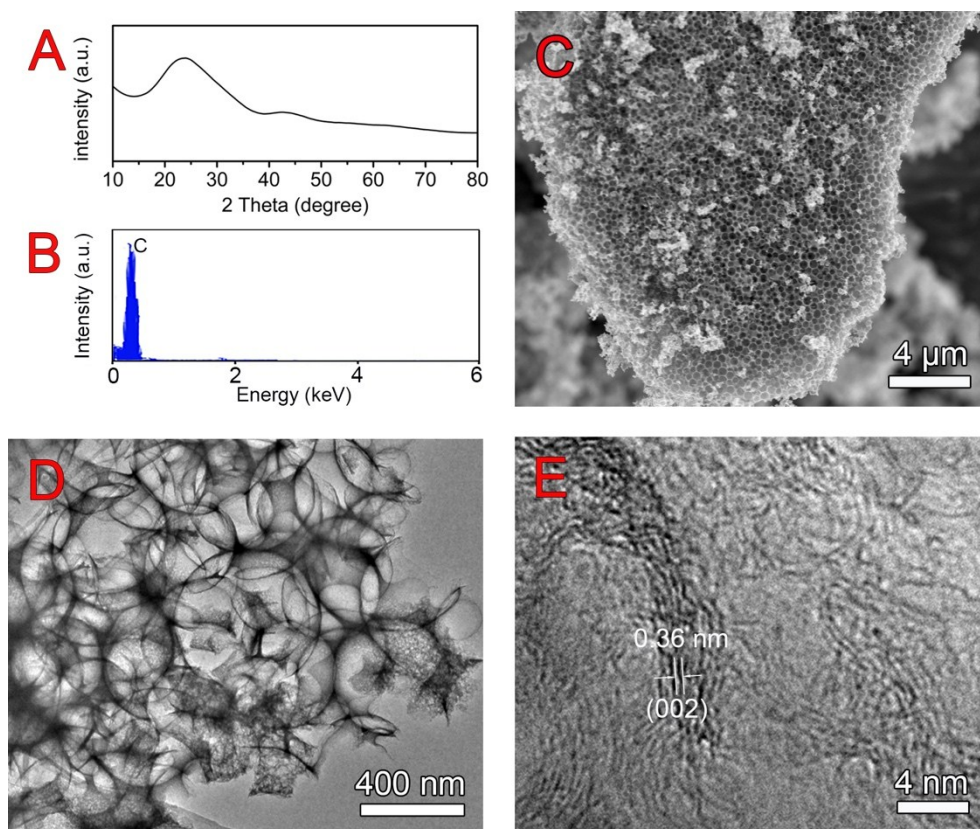


Figure S2. (A) XRD pattern, (B) EDX spectrum, (C) SEM image, (D) TEM image, and (E) HRTEM image of HCC.

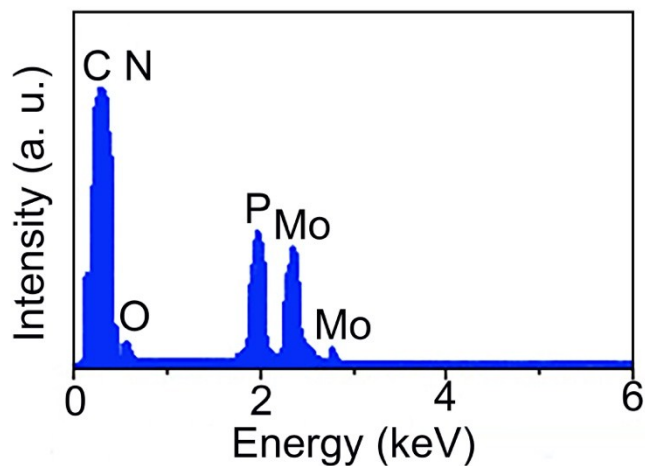


Figure S3. EDX spectra of MoP@HCC.

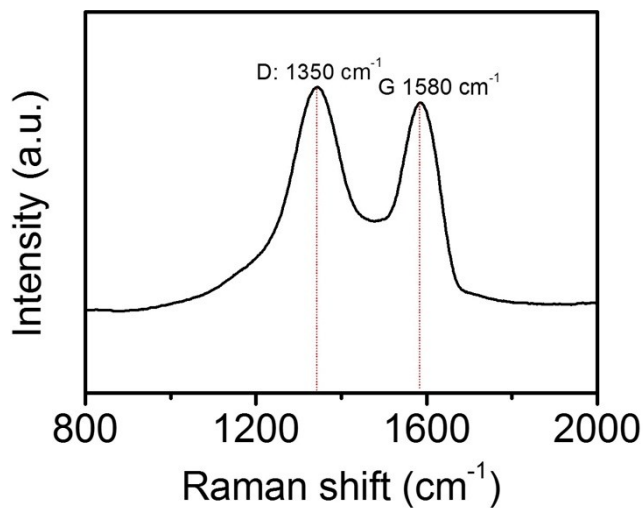


Figure S4. Raman spectra of MoP@HCC. The D-band and G-band correspond to the disordered graphitic carbon and graphitic carbon, respectively. The lower intensity of G-band with respect to D-band indicates the partially amorphous nature of the carbon component.

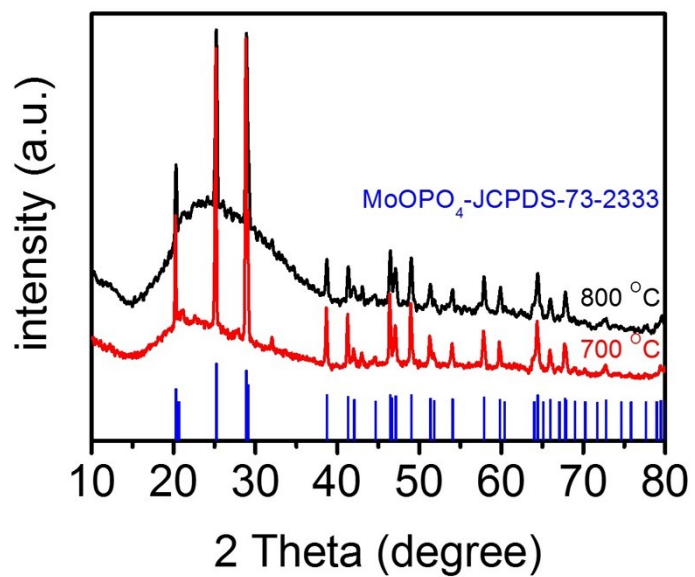


Figure S5. XRD pattern after TGA measurements in the air. After TGA measurements, all MoP were converted to MoOPO₄.

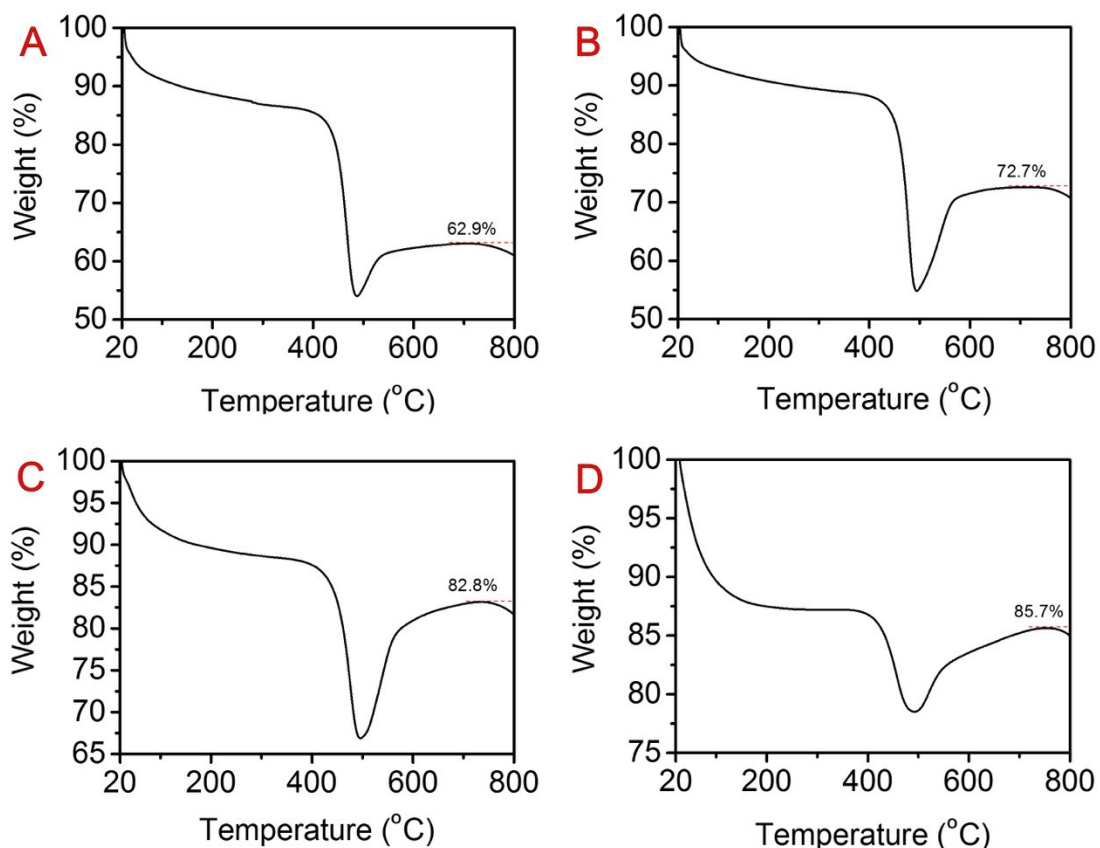


Figure S6. (A-D) TG analysis of MoP@HCC-(1-4) under high-purity air atmosphere at 1 °C/min.

To determine MoP content from TG curves, we assume that the samples consist of only MoP and carbon, and after heating to 800 °C in air, MoP is totally converted to MoOPO₄ and all the carbon-based materials have been completely burned. The MoP content is estimated according to the following equations:

$$m_{\text{MoP}}\% = m_{\text{residual mass}}\% \times M(\text{MoP}) / (M(\text{MoOPO}_4)).$$

For MoP@HCC, $m_{\text{MoP}}\% = 76.6\% \times 127/207 = 47.0\%$.

For MoP@HCC-1, $m_{\text{MoP}}\% = 62.9\% \times 127/207 = 38.6\%$.

For MoP@HCC-2, $m_{\text{MoP}}\% = 72.7\% \times 127/207 = 44.6\%$.

For MoP@HCC-3, $m_{\text{MoP}}\% = 82.8\% \times 127/207 = 50.8\%$.

For MoP@HCC-4, $m_{\text{MoP}}\% = 85.7\% \times 127/207 = 52.6\%$.

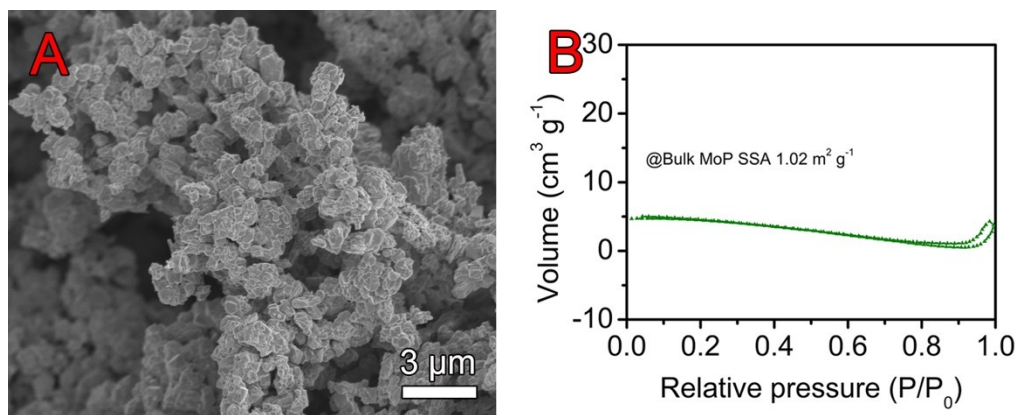


Figure S7. (A) SEM image and (B) N₂ adsorption-desorption isotherms of bulk MoP.

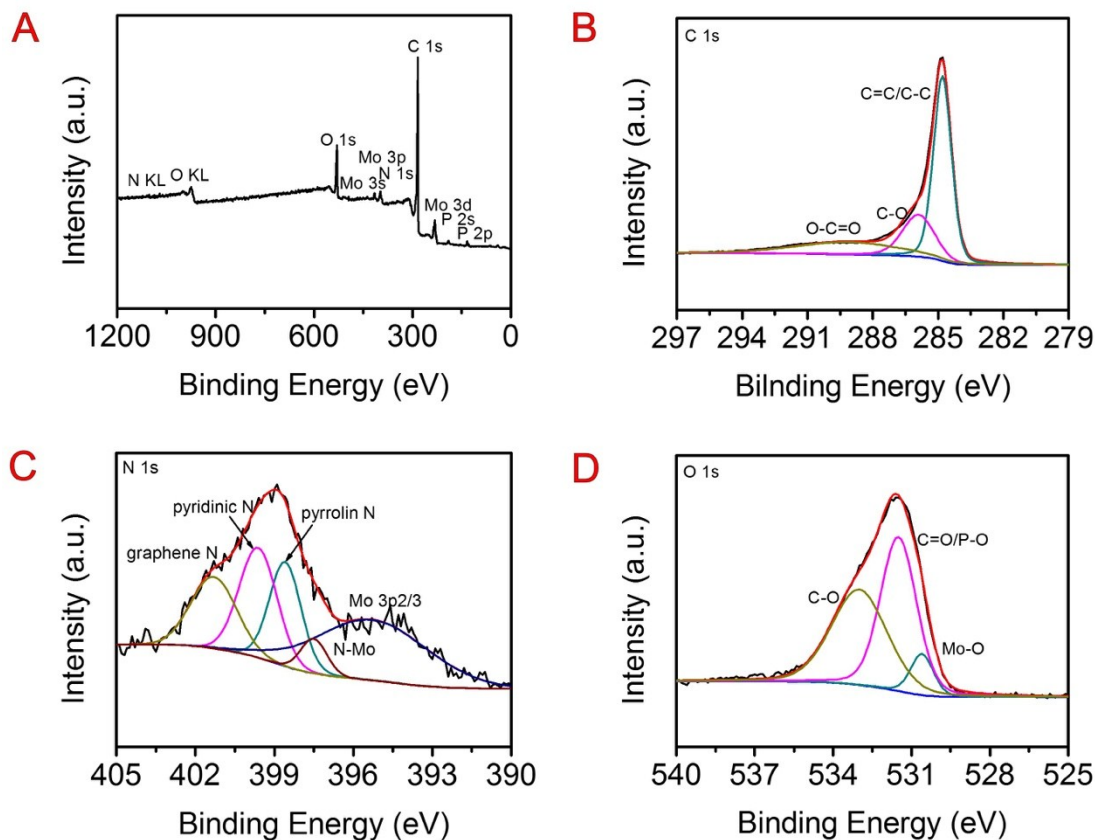


Figure S8. (A) XPS survey spectrum of MoP@HCC and deconvoluted core level spectra of (B) C 1s, (C) N 1s, and (D) O 1s.

The X-ray photoelectron spectroscopy (XPS) could be used to characterize the valence state and composition. Figure S8A show that the MoP@HCC was composed of C, N, O, Mo, and P elements, respectively. Figure S8B presents the high-resolution C1s XPS. The main peak at 284.8 eV indicates that the graphite carbon is the majority. The C-O and O-C=O bonds at 285.9 eV and 289.1 eV, respectively, were also found in C 1s spectrum. Figure S8C presents the high-resolution N 1s XPS. The deconvoluted bands at 398.3 eV, 399.7 eV, 401.3 eV can be assigned to pyridinic,

pyrrolic and graphene type N, respectively. A specific binding energy situating at 397.5 eV stood for N-Mo bond and a shoulder peak at 395.3 eV can be attributed to Mo $3p_{3/2}$.² Figure S8D presents the high-resolution O 1s XPS, which could be fitted into three components. The peaks at 531.5 eV and 533.2 eV are resulted from C=O/P-O and O-C bonds, respectively, which agree with C 1s and P 2p XPS, and the peak at 530.5 eV arises from the Mo-O bond.³

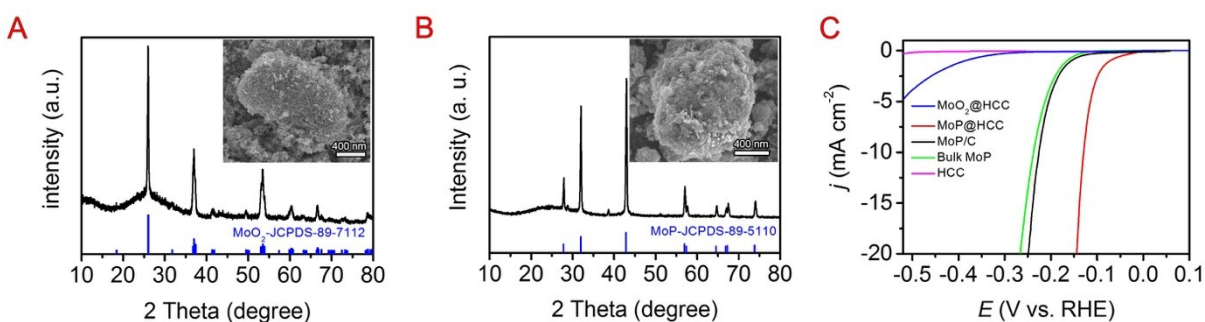


Figure S9. XRD patterns of MoO₂@HCC (A) and MoP/C (B); insets are corresponding SEM images. (C) HER polarization curves for MoP@HCC in comparison with MoP/C, bulk MoP, MoO₂@HCC, and HCC at a scan rate of 5 mV s⁻¹.

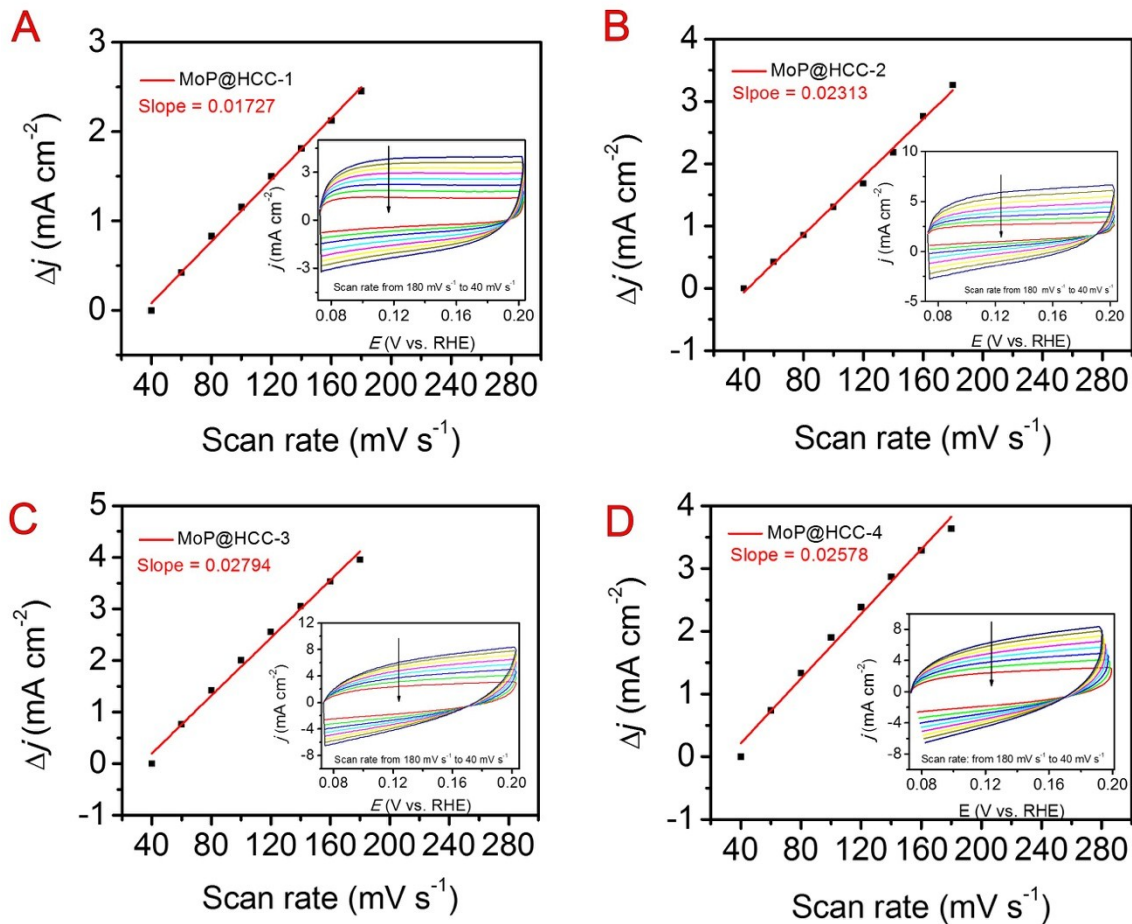


Figure S10. (A-D) Plots of the capacitive currents as a function of scan rate of MoP@HCC. The inset is the CVs.

Calculation of ECSA. Based on the linear fitting of Figure 4D, we can derive its specific capacitance as follows:

$$C = k / m, \text{ ECSA} = C / 60 \mu\text{F cm}^{-2}$$

Where C is the specific capacitance of MoP@HCC, k is the fitting slope, and m is the catalyst areal loading. ECSA can be calculated by assuming a standard value of $60 \mu\text{F cm}^{-2}$.⁴

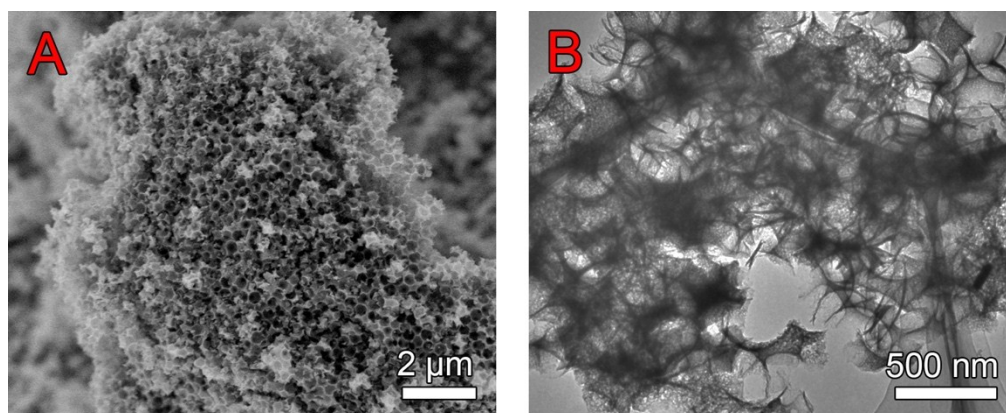


Figure S11. (A) SEM image and (B) TEM image of the MoP@HCC after long-term stability test.

Table S1. Comparison of representative HER catalysts in 0.5 M H₂SO₄.

Electrocatalyst	Substrate	Loading (mg cm ⁻²)	$\eta@10$ mA cm ⁻² (mV)	Tafel slope (mVdec ⁻¹)	Refs.
CoP/CNT	GCE	0.285	122	54	5
CoP nanowire arrays	CC	0.92	67	51	6
CoP nanoparticles	Ti foil	0.9	88	48	7
Ni-P	CP	25.8	98	59	8
Ni ₂ P/CNT	GCE	0.184	124	41	9
WP ₂	GCE	/	148	52	10
FeP nanotubes	CC	1.6	88	36	11
Fe ₂ P/NGr	GCE	1.71	138	/	12
Mo ₂ C@NC	GCE	0.28	124	60	13
P-WN/rGo	GCE	0.28	124	60	14
SV-MoS ₂	Au	/	170	60	15
MoP@PC	GCE	0.41	153	66	2
MoP@CA2	GCE	0.36	125	54	16
MoP@HCC	GCE	0.26	129	48	This work

References

1. Q. Yu, P. Wang, S. Hu, J. Hui, J. Zhuang and X. Wang, *Langmuir*, 2011, **27**, 7185-7191.
2. J. Yang, F. Zhang, X. Wang, D. He, G. Wu, Q. Yang, X. Hong, Y. Wu and Y. Li, *Angew. Chem.-Int. Edit.*, 2016, **55**, 12854-12858.
3. Y. J. Tang, M. R. Gao, C. H. Liu, S. L. Li, H. L. Jiang, Y. Q. Lan, M. Han and S. H. Yu, *Angew. Chem.-Int. Edit.*, 2015, **54**, 12928-12932.
4. J. Wang, W. Wang, L. Ji, S. Czioska, L. Guo and Z. Chen, *ACS Appl. Energy Mater.*, 2018, **1**, 736-743.
5. Q. Liu, J. Tian, W. Cui, P. Jiang, N. Cheng, A. M. Asiri and X. Sun, *Angew. Chem.-Int. Edit.*, 2014, **53**, 6710-6714.
6. J. Tian, Q. Liu, A. M. Asiri and X. Sun, *J. Am. Chem. Soc.*, 2014, **136**, 7587-7590.
7. D.-H. Ha, B. Han, M. Risch, L. Giordano, K. P. C. Yao, P. Karayaylali and Y. Shao-Horn, *Nano Energy*, 2016, **29**, 37-45.
8. X. Wang, W. Li, D. Xiong, D. Y. Petrovykh and L. Liu, *Adv. Funct. Mater.*, 2016, **26**, 4067-4077.
9. Y. Pan, W. Hu, D. Liu, Y. Liu and C. Liu, *J. Mater. Chem. A*, 2015, **3**, 13087-13094.

10. H. Du, S. Gu, R. Liu and C. M. Li, *J. Power Sources*, 2015, **278**, 540-545.
11. Y. Yan, B. Y. Xia, X. Ge, Z. Liu, A. Fisher and X. Wang, *Chemistry*, 2015, **21**, 18062-18067.
12. Z. Huang, C. Lv, Z. Chen, Z. Chen, F. Tian and C. Zhang, *Nano Energy*, 2015, **12**, 666-674.
13. Y. Liu, G. Yu, G. D. Li, Y. Sun, T. Asefa, W. Chen and X. Zou, *Angew. Chem.-Int. Edit.*, 2015, **54**, 10752-10757.
14. H. Yan, C. Tian, L. Wang, A. Wu, M. Meng, L. Zhao and H. Fu, *Angew. Chem.-Int. Edit.*, 2015, **54**, 6325-6329.
15. H. Li, C. Tsai, A. L. Koh, L. Cai, A. W. Contryman, A. H. Fragapane, J. Zhao, H. S. Han, H. C. Manoharan, F. Abild-Pedersen, J. K. Nørskov and X. Zheng, *Nat. Mater.*, 2016, **15**, 364.
16. Z. Xing, Q. Liu, A. M. Asiri and X. Sun, *Adv. Mater.*, 2014, **26**, 5702-5707.